2013 European Control Conference (ECC)
July 17-19, 2013, Zürich, Switzerland.

# Constrained real-time optimal control for cyclic AC PWM systems

Claudia Fischer, Sébastien Mariéthoz, Manfred Morari

*Abstract*— **The paper introduces a constrained optimal control approach for cyclic AC PWM systems for which computation of the optimal modulation with respect to some cost criterion is too complex for real-time execution. For such systems it is possible to precompute optimal cyclic steady state solutions for different operating points and create a look-up table for real-time implementation. As the operating point changes, direct application of the corresponding optimal cyclic steady state solution causes adverse effects, such as increased system losses. The proposed optimal control approach allows to reduce these effects by doing fast transitions between precomputed optimal solutions, bringing the system to the new optimal steady state operation within half a cycle. The approach effectiveness is demonstrated on a multisource DC-DC converter benchmark example.**

## I. Introduction

Power electronics systems combine passive devices with continuous time dynamics and actively controlled switching devices. Due to the limitations and losses associated with the transition of switching devices, the switching frequency needs to be limited. This is often ensured by generating the switch control signals with pulse-width modulators. The manipulated variables then are the discrete time variables that describe the switching on and off instants. In the commonly used averaging approach it is typically assumed that these variables enter the system linearly, allowing for synthesis of simple controllers.

By doing this approximation, however, important information is lost about the switched trajectories, only the average behaviour of the system can be controlled. The resulting model cannot be used to evaluate the switching ripple or conversion losses. Recent work on hybrid optimal and model predictive control (MPC) using models that capture the switched behaviour of the system has been dealing with problems such as reducing the tracking error including the distortion caused by the switching [1]–[5]. Formulating the MPC problem with a quadratic objective using piece-wise affine and mixed-logical dynamic models result in mixed integer quadratic programs. This limits the number of switches and the length of the horizon for which the problem can be solved in real-time at frequencies in the kHz range.

Due to the switched operation the system has in general no equilibrium, but the steady-state cycle that optimises the control objective is sought. In AC-DC power converters, the steady-state cycle duration is equal to the converter AC frequency. The optimisation problem with the corresponding horizon cannot be computed in real-time at the necessary frequencies. In [6], the authors compute the steady state cycles offline for a set of operating modes, and build a look-up table to find the relevant the steady state cycle to be applied in real-time using interpolation. The heuristic proposed in [7] is then applied to reduce the detrimental effects that appear during transitions between different operating points.

The present paper proposes to replace this heuristic by an optimisation based control scheme for fast transitions between precomputed steady state cycles for AC systems.

The paper is organised as follows. Section II describes the modelling of AC PWM systems. In section III the precomputation of the optimal cyclic steady state solutions is discussed. In section IV the control approach is introduced and feasibility conditions for the optimal control problem are given. Section V deals with the application of the approach to multisource converters. Finally, the control performance for two different instances of the control approach is assessed in simulation for a threesource converter in section VI.

## II. Modelling of AC PWM systems

The systems considered in this paper are systems with the following dynamics

$$\dot{\boldsymbol{x}}(t) = \boldsymbol{F}\boldsymbol{x}(t) + \boldsymbol{G}\boldsymbol{s}(t) \tag{1a}$$

$$\boldsymbol{y}(t) = \frac{1}{T_\mathrm{p}} \int_{t-T_\mathrm{p}}^{t} \boldsymbol{\rho}(\boldsymbol{x}(\tau), \boldsymbol{s}(\tau)) d\tau \tag{1b}$$

where $\boldsymbol{s}(t)$ is in the set of PWM signals. PWM functions are switched functions with a limit on the number of transitions the signals can make during a predefined time interval. Therefore, PWM systems do not reach an equilibrium but a cyclic steady state solution, here with cycle period $T_\mathrm{p}$. The output $\boldsymbol{y}(t)$ is defined as a functional $\boldsymbol{\rho}(\boldsymbol{x}(t), \boldsymbol{s}(t))$ over such a cycle.

This paper deals with AC PWM systems. These are PWM systems whose cyclic steady state solutions have the following properties:

$$\boldsymbol{x}^*(t) = \boldsymbol{x}^*(t + T_\mathrm{p}) = -\boldsymbol{x}^*(t + \frac{T_\mathrm{p}}{2}) \tag{2a}$$

$$\boldsymbol{s}^*(t) = \boldsymbol{s}^*(t + T_\mathrm{p}) = -\boldsymbol{s}^*(t + \frac{T_\mathrm{p}}{2}). \tag{2b}$$

Hence, the PWM function has to be able to take positive as well as negative values.

### A. Modelling of three-level PWM functions

This section describes a way of modelling PWM functions that can take values in $\{-1, 0, 1\}$, so-called three-level PWM functions, and their corresponding constraints in continuous and discrete time.

The authors are with the Automatic Control Laboratory, Swiss Federal Institute of Technology Zurich (ETH), Zurich, Switzerland, Email: {fischer, mariethoz, morari}@control.ee.ethz.ch

*1) Continuous time model:* An important part in modelling three-level PWM functions is the fact that the number of signal transitions during a 'switching period' $T_\mathrm{s}$ is limited, as the switches in the physical system cannot be turned on and off arbitrarily fast. Thus, the vector of PWM signals $\boldsymbol{s}(t)$ is subject to according constraints.

Admissible patterns for any entry $s^j(t)$ of $\boldsymbol{s}(t)$ exhibit at most two up and two down transitions during a switching period $T_\mathrm{s}$, as displayed in Fig. 1. The order of these

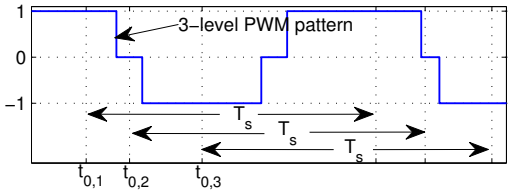


Fig. 1. Admissible input patterns for $s^j(t)$ have at most two up and two down transitions during a switching period $T_\mathrm{s}$ for any initial value $t_{0,i}$.

transitions and hence the constraints on $\boldsymbol{s}(t)$ depend on the initial value of the pattern $s^j(t_0)$ and must be such that $s^j(t) \in \{-1, 0, 1\}\ \forall t$.

Such patterns can be represented using four Heaviside functions $h(t - t^{j,i})$ per switching period, the initial value of the pattern $s^j(t_0)$, and constraints on $s^j(t)$. For simplified notation $t_0$ is chosen to be 0. A three-level PWM pattern for $n_p$ switching periods is modelled as

$$\begin{aligned} s^j(t) &= s^j(0) + \sum_{i=1}^{2n_p} (-1)^{i+1} \left( h(t - t^{j,2i-1}) - h(t\ - t^{j,2i}) \right) \\ &:= s^j(0) + \sum_{i=1}^{n_h} M_{ji} h(t - t^{j,i}) \end{aligned} \tag{3a}$$

$$s^j(t) \in \{-1, 0, 1\},\ t \in [0, n_p T_\mathrm{s}) \tag{3b}$$

$$t^{j,i} \in [0, n_p T_\mathrm{s})\ \forall (j,i) \in \{1, \ldots, n_s\} \times \{1, \ldots, 4n_p\} \tag{3c}$$

where $n_h = 4n_p n_s$ the total number of Heaviside functions, and $\boldsymbol{M} \in \{-1, 0, 1\}^{n_s \times n_h}$ is an auxiliary matrix for more compact notation.

*Remark:* The above model can straightforwardly be extended to general m-level PWM functions that take integer values in $[-\frac{m}{2}, \ldots, \frac{m}{2}]$ by increasing the number of Heaviside functions and augmenting the feasible set for $s^j(t)$ accordingly.

*2) Discrete time model:* An optimisation problem that features the above dynamics is hard to solve, as the model of the PWM patterns given in (3) is a nonlinear and nonconvex function of the transition times $t^{j,i}$. By discretising the system it is possible to formulate an optimisation problem that results in a mixed integer quadratic problem (MIQP). To find a discrete time representation of the PWM function, the time $n_p T_\mathrm{s}$ is divided into $q$ intervals, resulting in a discretisation period of $T_\mathrm{q} = \frac{n_p T_\mathrm{s}}{q}$.

To model the control input and its constraints (3) in discrete time, the Heaviside functions are represented by their normalised integral over each discretisation period:

$$h_k^{j,i} = \frac{1}{T_\mathrm{q}} \int_{kT_\mathrm{q}}^{(k+1)T_\mathrm{q}} h(t - t^{j,i}) dt \tag{4a}$$

A remarkable property of this discretisation is that the transition times $t^{j,i}$ can be recovered easily:

$$t^{j,i} = T_\mathrm{q} \sum_{k=0}^{q-1} (1 - h_k^{j,i}) \tag{4b}$$

This property is useful for the physical implementation of the controller as the control input can be parametrised straightforwardly in terms of these transition times.

To be able to incorporate this into a discrete time optimisation problem, equation (4a) can equivalently be represented using a binary variable $\delta_k^{j,i}$, that takes the value 1 in the interval where the switch transition occurs and 0 otherwise, and a continuous variable $d_k^{j,i}$ that models the value of the discrete representation of the Heaviside function $h^{j,i}$ during the transition interval and is 0 othervise . Thus, $\boldsymbol{s}_k$ is a piecewise constant represenation of $\boldsymbol{s}(t)$. The discrete time representation of (3) can be written as

$$\boldsymbol{s}_k = \boldsymbol{s}(0) + \boldsymbol{M}\boldsymbol{h}_k \tag{5a}$$

$$\boldsymbol{h}_k = \left( \sum_{l=0}^{k-1} \boldsymbol{\delta}_l \right) + \boldsymbol{d}_k \tag{5b}$$

$$\mathbf{0} \leq \boldsymbol{d}_k \leq \boldsymbol{\delta}_k \tag{5c}$$

$$\sum_{k=0}^{q-1} \boldsymbol{\delta}_k \leq \mathbf{1} \tag{5d}$$

$$\boldsymbol{\delta}_k \in \{0,1\}^{n_h},\ \boldsymbol{d}_k \in [0,1]^{n_h},\ \boldsymbol{s}_k \in [-1,1]^{n_s}. \tag{5e}$$

### *B. Discrete time system dynamics*

The discrete time model of (1) is obtained by employing the discrete time representation of $\boldsymbol{s}_k$ into the linear dynamic equations. The discrete time system dynamics are

$$\boldsymbol{x}_{k+1} = e^{\boldsymbol{F}T_\mathrm{q}} \boldsymbol{x}_k + \int_0^{T_\mathrm{q}} e^{\boldsymbol{F}(T_\mathrm{q} - \tau)} d\tau \boldsymbol{G} \boldsymbol{s}_k \tag{6a}$$

$$:= \boldsymbol{A}\boldsymbol{x}_k + \boldsymbol{B}\boldsymbol{s}_k \tag{6b}$$

$$\boldsymbol{y}_k = \frac{1}{q} \sum_{j=k+1-q}^{k} \boldsymbol{r}(\boldsymbol{x}_j, \boldsymbol{s}_j). \tag{6c}$$

where $\boldsymbol{s}_k$ as defined in (5), and $\boldsymbol{g}_\mathrm{q}$ a piece-wise affine function of $\boldsymbol{x}$ and $\boldsymbol{s}$.

## III. Optimal cyclic solutions of AC PWM systems

A case of particular interest is the class of AC PWM systems where infinitely many PWM pattern yield the same system output $\boldsymbol{y}$. In that case it is possible to formulate an optimisation problem to find the best PWM pattern that yields a desired $\boldsymbol{y}_\mathrm{ref}$ and minimises a given cost criterion.

As the discretised dynamics feature integer variables, such an optimisation problem results in a mixed-integer problem. This is too complex to solve in real-time in a power converter,

as their switching frequency is in the range of tens or hundreds of kHz. It is however possible to precompute the optimal cyclic steady state solutions for different operating points defined by $\boldsymbol{y}_{\mathrm{ref}}$.

In [6] the authors describe a systematic way of precomputing such cyclic steady state solutions for minimum conversion losses given a desired reference power transfer. The approach is applied to the class of multisource DC-DC power converters, resulting in superior performance compared to state of the art control schemes at steady state operation.

## IV. Control approach

The challenge addressed in the present paper is how to make transitions between these precomputed steady state solutions as the operating point $\boldsymbol{y}_{\mathrm{ref}}$ changes. The concept of the control approach introduced is to reach the new optimal steady state quickly and without large transients in state or output, after a change in the desired operating point. In this section it is shown that under certain conditions it is possible to make the transition between any two precomputed cyclic steady state solutions within half a cycle.

### A. Optimal control problem

We define a finite horizon optimal control problem for a transition from $\boldsymbol{y}^1_{\mathrm{ref}}$ to $\boldsymbol{y}^2_{\mathrm{ref}}$ with respective optimal cylcic steady state solutions $(\boldsymbol{x}^{*1}(t), \boldsymbol{s}^{*1}(t))$ and $(\boldsymbol{x}^{*2}(t), \boldsymbol{s}^{*2}(t))$ with corresponding transition functions $\boldsymbol{h}^{*1,2}(t)$ within half a cycle period, i.e. within $\frac{q}{2}$ steps where $q$ is an even number:

$$\min_{\boldsymbol{h}_0,\ldots,\boldsymbol{h}_{q-1}} \sum_{k=0}^{q-1} \left(\boldsymbol{h}_k - \boldsymbol{h}_k^{*2}\right)^T \boldsymbol{R} \left(\boldsymbol{h}_k - \boldsymbol{h}_k^{*2}\right) + \\ + \left(\boldsymbol{y} - \boldsymbol{y}^2_{\mathrm{ref}}\right)^T \boldsymbol{Q}_{\boldsymbol{y}} \left(\boldsymbol{y} - \boldsymbol{y}^2_{\mathrm{ref}}\right) \tag{7a}$$

$$\text{s.t. discrete time system dynamics as in (6)} \tag{7b}$$

$$\boldsymbol{x}_0 = \boldsymbol{x}^{*1}(0) \tag{7c}$$

$$\boldsymbol{x}_{\frac{q}{2}} = \boldsymbol{x}^{*2}(\frac{T_{\mathrm{p}}}{2}) \tag{7d}$$

$$\boldsymbol{s}^{*1}(0) + \sum_{k=0}^{\frac{q}{2}-1} \boldsymbol{M}\boldsymbol{\delta}_k = \boldsymbol{s}^{*2}(\frac{T_{\mathrm{p}}}{2}) \tag{7e}$$

$$\boldsymbol{s}_k,\ \boldsymbol{\delta}_k \text{ as in (5)} \tag{7f}$$

where $\boldsymbol{M}\boldsymbol{\delta}_k$ represents the change of the physical position of the switches during discretisation interval $k$. $\boldsymbol{R} > 0$ ensures implementation of the precomputed steady state solution if $\boldsymbol{y}^1_{\mathrm{ref}} = \boldsymbol{y}^2_{\mathrm{ref}}$, and $\boldsymbol{Q}_{\boldsymbol{y}} \geq 0$ enables operation close to the new reference during transient.

Due to the constraints (7d) and (7e), problem (7) is not feasible in general. In the next section, a feasibility condition that is easy to check, is derived.

### B. Feasibility of the optimal control problem

To check feasibility of the optimal control problem, it is sufficient to check whether $\boldsymbol{x}^{*\mathbf{2}}(\frac{T_{\mathrm{p}}}{2})$ can be reached from any $\boldsymbol{x}^{*\mathbf{1}}(0)$ within time $\frac{T_{\mathrm{p}}}{2}$. The input is subject to switching constraints (7e) and (7f). For notational simplicity, in the following it is assumed that the impact of constraint (7e) is the same for all precomputed optimal solutions. Extension to the more general setup is straightforward by distinguishing the different cases.

Starting from an initial $\boldsymbol{x}_0$, the reachable set $R_{x_0}$ is

$$R_{x_0} := \left\{ \boldsymbol{x} | \boldsymbol{x} = e^{\boldsymbol{F}\frac{T_{\mathrm{p}}}{2}}\boldsymbol{x}_0 + \int_0^{\frac{T_{\mathrm{p}}}{2}} e^{\boldsymbol{F}(\frac{T_{\mathrm{p}}}{2}-\tau)} d\tau \boldsymbol{G}\boldsymbol{s}(0) + \right. \\ \left. \sum_{i=1}^{n_T} \sum_{j\in J_i} \int_{t^{j,i}}^{iT} e^{\boldsymbol{F}(iT-\tau)} \tilde{g}_j d\tau, t^{j,i} \in [(i-1)T, iT] \right\}. \tag{8a}$$

$\frac{T_{\mathrm{p}}}{2}$ is split into $n_T$ intervals of duration $T$. $J_i$ are sets of the indices of the transitions happening in $[(i-1), i]T$. $T$ and $J_i$ are selected such that the switching constraints are obeyed. $\tilde{g}_j$ is a row of $\boldsymbol{GM}$ that determines the influence of the transition function on the state $\boldsymbol{x}$.

The set $R_{x_0}$ is in general non-convex. In order to find a feasibility certificate that is easy to check, a convex inner approximation of $R(\boldsymbol{x}(0))$ is sought. Thereto, the Taylor expansion of the matrix exponential is computed, yielding

$$R_{x_0} = \left\{ \boldsymbol{x} | \boldsymbol{x} = e^{\boldsymbol{F}\frac{T_{\mathrm{p}}}{2}}\boldsymbol{x}_0 \int_0^{\frac{T_{\mathrm{p}}}{2}} e^{\boldsymbol{F}(\frac{T_{\mathrm{p}}}{2}-\tau)} d\tau \boldsymbol{G}\boldsymbol{s}(0) + \right. \\ \left. \sum_{i=1}^{n_T} \sum_{j\in J_i} \left( \underbrace{(iT - t^{j,i})}_{linear} + \underbrace{\sum_{k=1}^{\infty} \frac{\boldsymbol{F}^k (iT - t^{j,i})^{k+1}}{(k+1)!}}_{nonlinear} \right) \tilde{g}_j, \right. \\ \left. t^{j,i} \in [(i-1)T, iT] \right\}. \tag{8b}$$

The nonlinear term takes its maximum where $(iT - t^{j,i})$ is maximum, i.e. where $(iT - t^{j,i}) = T$. Hence, a bound for the nonlinear term can be computed based on the diagonal decomposition of $\boldsymbol{F}$, $\boldsymbol{F} = \boldsymbol{V}\boldsymbol{\Lambda}\boldsymbol{V}^{-1}$:

$$||\tilde{\boldsymbol{F}}|| = ||\boldsymbol{V}\left(\boldsymbol{\Lambda}^{-1}(e^{\boldsymbol{\Lambda}T} - \boldsymbol{I}) - T\boldsymbol{I}\right)\boldsymbol{V}^{-1}|| \tag{8c}$$

$$\leq \max(|\lambda(\tilde{\boldsymbol{F}})|) \tag{8d}$$

An inner convex estimation of the reachable set $\tilde{R}_{x_0}$ is

$$\tilde{R}_{x_0} = \left\{ \boldsymbol{x} | \boldsymbol{x} = e^{\boldsymbol{F}\frac{T_{\mathrm{p}}}{2}}\boldsymbol{x}_0 \int_0^{\frac{T_{\mathrm{p}}}{2}} e^{\boldsymbol{F}(\frac{T_{\mathrm{p}}}{2}-\tau)} d\tau \boldsymbol{G}\boldsymbol{s}(0) + \right. \\ \left. \sum_{i=1}^{n_T} \sum_{j\in J_i} (iT - t^{j,i}))\tilde{g}_j, t^{j,i} \in [(i-1)T, iT] \right\} \\ \ominus \left\{ \boldsymbol{x} | \boldsymbol{x} \leq n_T \max(|\lambda(\tilde{\boldsymbol{F}})|) \sum_{j\in J_i} |\tilde{g}_j| \right\} \tag{8e}$$

where $\ominus$ is the Minkowski difference of the two sets. As the term $e^{\boldsymbol{F}\frac{T_{\mathrm{p}}}{2}}\boldsymbol{x}_0 \int_0^{\frac{T_{\mathrm{p}}}{2}} e^{\boldsymbol{F}(\frac{T_{\mathrm{p}}}{2}-\tau)} d\tau \boldsymbol{G}\boldsymbol{s}(0)$ does not depend

on $t^{i,j}$, a new set is defined:

$$\tilde{R} := \left\{ \boldsymbol{x} | \boldsymbol{x} = \sum_{i=1}^{n_T} \sum_{j \in J_i} (iT - t^{j,i}))\tilde{g}_j, t^{j,i} \in [(i-1), iT] \right\} \ominus \left\{ \boldsymbol{x} | \boldsymbol{x} \leq n_T \max(|\lambda(\tilde{\boldsymbol{F}})|) \sum_{j \in J_i} |\tilde{g}_j| \right\} \tag{8f}$$

To assess the feasibility of the optimal control problem (7), it is sufficient to check if for all vertices $(\boldsymbol{x}^{*1}(t), \boldsymbol{s}^{*1}(t))$ and $(\boldsymbol{x}^{*2}(t), \boldsymbol{s}^{*2}(t))$ of the set of precomputed cyclic steady state solutions, it holds that

$$\boldsymbol{x}^{*1}(\frac{T_\mathrm{p}}{2}) - \left( e^{\boldsymbol{F}\frac{T_\mathrm{p}}{2}} \boldsymbol{x}^{*1}(0) \int_0^{\frac{T_\mathrm{p}}{2}} e^{\boldsymbol{F}(\frac{T_\mathrm{p}}{2} - \tau)} d\tau \boldsymbol{G} \boldsymbol{s}^{*1}(0) \right) \in \tilde{R} \tag{8g}$$

This condition can be checked easily using the computational geometry package of the MPT toolbox. [8]

## V. Application to Multisource Power Converters

The proposed optimal control formulation can now be applied to the class of DC-DC multisource power converters. They control the transfer of power or energy between several

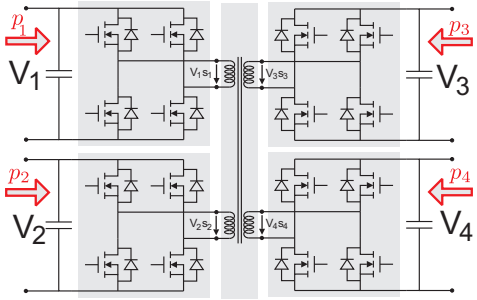


Fig. 2. Multisource converter with four sources.

DC sources that need to be isolated or operate at significantly different voltages. An example of such a multisource converter with four sources is given in Fig. 2. The sources are connected to and exchange energy over only one common multiwinding transformer.

To be able to apply the introduced control approach, first the continuous time control model is derived and discretised. This then serves as a basis to approximate the power transfer.

### A. System dynamics

The differential equations that describe the system dynamics of the investigated converter topology are derived from its equivalent electric circuit given in Fig. 3. The states $\boldsymbol{x}(t)$ of the system are the electric currents $i_j$, the inputs are the three-level PWM functions $\boldsymbol{s}(t)$, that represent the signs of the voltages. The inductances $L_j$ as well as the voltages $V_j$ are assumed to be constant.

The continuous time system dynamics are as in (1) with $n_x = n_s$, $\boldsymbol{x}(t) \in \mathbb{R}^{n_x}$, $\boldsymbol{F} = \boldsymbol{0}^{n_x \times n_x}$, and $\boldsymbol{G} \in \mathbb{R}^{n_x \times n_s}$. $\boldsymbol{G} = \hat{\boldsymbol{G}}(\boldsymbol{V} \dots \boldsymbol{V})^T)$ where $\boldsymbol{V}$ is the column vector of source voltages. The entries of $\hat{\boldsymbol{G}}$ are $\hat{\boldsymbol{G}}_{ii} = \left( L_i + \left( \sum_{j \neq i} \frac{1}{L_j} \right)^{-1} \right)^{-1}$, and $\hat{\boldsymbol{G}}_{ij} = -\frac{\hat{\boldsymbol{G}}_{jj}}{L_i} \left( \sum_{j \neq i} \frac{1}{L_j} \right)^{-1}$. $\boldsymbol{s}(t)$ is a vector of three-level PWM functions as in (3). The discrete time system dynamics can be modelled as in (6).

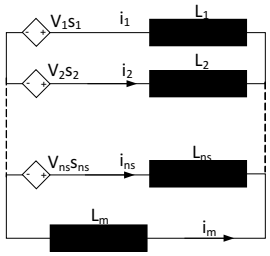


Fig. 3. Equivalent circuit of the general multisource converter with $n_s$ sources.

### B. Power transfer

The discretised system dynamics are used to model of the transmitted power, the system output. This is used for output tracking during transient. The transmitted power $y^j$ that is associated with state $x^j$ and input $s^j$ is defined as the average of the instantaneous power during half a cycle period. Here, the cycle period and the switching period coincide, i.e. $T_\mathrm{p} = T_\mathrm{s}$. The power equation and its approximation using (5a) are:

$$y^j := \frac{2}{q} \sum_{k=0}^{\frac{q}{2}-1} \frac{1}{2} (x_k^j + x_{k+1}^j) V^j s_k^j \tag{10a}$$

$$\approx \frac{V^j}{q} \sum_{k=0}^{\frac{q}{2}-1} s^j(0)(x_k^j + x_{k+1}^j) + \boldsymbol{M_j}. \left( \sum_{l=0}^{k-1} \boldsymbol{x}_l^{j,\delta} + \boldsymbol{x}_k^d \right) \tag{10b}$$

where $\boldsymbol{M_j}.$ denotes the $j^{th}$ row of matrix $\boldsymbol{M}$, $\boldsymbol{x}_k^d$ is a piecewise affine approximation of $(x_k^j + x_{k+1}^j)\boldsymbol{d}_k$, and $\boldsymbol{x}_l^{j,\delta}$ is an exact representation of the product $(x_k^j + x_{k+1}^j)\boldsymbol{\delta}_l$, defined as

$$\underline{x}^j \boldsymbol{\delta}_l \leq \boldsymbol{x}_l^{j,\delta} \leq \overline{x}^j \boldsymbol{\delta}_l \tag{10c}$$

$$\underline{x}^j (\boldsymbol{1} - \boldsymbol{\delta}_l) \leq \boldsymbol{x}_l^{j,\delta} - (x_k^j + x_{k+1}^j) \leq \overline{x}^j (\boldsymbol{1} - \boldsymbol{\delta}_l) \tag{10d}$$

with $\underline{x}^j$ a lower, and $\overline{x}^j$ an upper bound on $(x_k^j + x_{k+1}^j)$.

Note that $\boldsymbol{M_j}.\boldsymbol{d}_k$ are non-zero only at two instances of $k$ during the horizon. Using a finer discretisation grid increases the accuracy of the approximation.

### C. Optimal cyclic solutions

For every operating point defined by the vector of power transmission $\boldsymbol{y}_\mathrm{ref}$ at each source, an optimal cyclic steady state solution with period $T_\mathrm{p}$ that yields minimum losses can be precomputed using the method described in [6]. The cycle period $T_\mathrm{p}$ coincides with the switching period $T_\mathrm{s}$. At steady state, the system is operated optimally with these precomputed cyclic inputs.

### D. Applicability of the proposed dynamic control scheme

For the control during transitions between precomputed cyclic solutions, the proposed scheme can be applied. The optimal precomputed solutions can be shifted such that the initial state of the switches is the same for all. Condition (8f) is verified using the MPT toolbox [8].

## VI. Simulation results

The system is simulated for $n_s = 3$, that is for a threesource converter. The leakage inductances are the same, $L_{1,2,3} = 116\mu$H. The mutual inductance is $L_m = 20L$. The switching frequency is 20kHz, resulting in a switching and cycle period $T_\mathrm{p} = 50\mu$s. The three source voltages are equal and constant, $V^{1,2,3} = 325$V. The maximum admissible total power transfer is 3kW. All simulations were run in MATLAB, using YALMIP [9] to formulate and GUROBI to solve the optimisation problems.

### A. Dynamic control schemes

For controlling the transitions between the optimal cyclic solutions, three different schemes are implemented and compared in simulation. The first scheme is a reference scheme where the optimal precomputed cyclic steady state solutions are applied directly to the system. The other two investigated controllers are based on two different instances of the proposed control approach.

*1) Reference scheme:* In the reference scheme the cyclic input corresponding to the new reference power is applied directly without taking additional measures when the operating point changes. This scheme is often used in practice.

*2) Input tracking controller formulation:* The input tracking controller results from formulating the optimisation problem (7) with $\boldsymbol{R} = \boldsymbol{I}$ and discretisation grid of $q = 2$. As no power tracking is performed, $\boldsymbol{Q_y} = \boldsymbol{0}$, the output computation is omitted. Thus, all integer variables are removed, and the optimisation problem for the input tracking controller results in a quadratic program (QP) that can be solved in real-time, [10].

*3) Power tracking controller formulation:* To formulate the optimisation problem for the power tracking controller, a discretisation grid of $q = 40$ is used to obtain a good model of the transmitted power. The optimisation problem results in an MIQP. The weight matrices are $\boldsymbol{R} = \boldsymbol{I}$, and $\boldsymbol{Q_y} = 1000\boldsymbol{I}$.

### B. Comparison of the dynamic control schemes

In Fig. 4 the performance of the three different schemes is compared for a change in power reference at time $T_\mathrm{p}$. The straightforward approach of directly applying the precomputed cyclic solutions results in a constant state displacement with respect to the optimal cyclic solution after the change in reference, that is, the mean of the state is no longer zero. Thus, the state has a component that does not contribute to the transmitted power, but increases the conversion losses and may cause saturation of the transformer. The dynamic performance of the input and the power tracking controllers are comparable in terms of the average value of the state and outperform the first approach. The average of the state

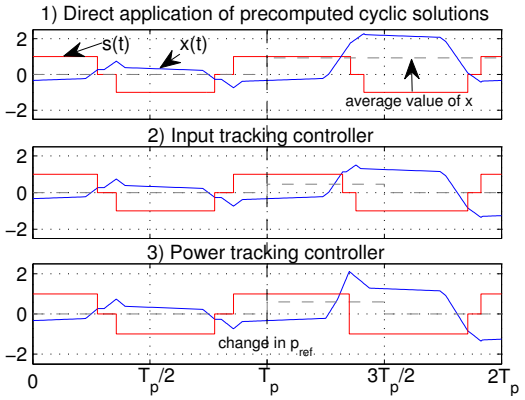


Fig. 4. Comparison of the dynamic performance of the three different controllers for a change of operating point at $T_\mathrm{p}$. Plots show state and input trajectories at source 2.

exhibits a small average value during the transition period $[T_\mathrm{p}, \frac{3T_\mathrm{p}}{2}]$, but as expected the system reaches the optimal cyclic state and input trajectories for the new operating point within half a switching period. The state and input waveforms observed for the input and power tracking controllers differ. This implies different losses and power tracking performance.

### C. Power tracking performance

Two benchmark tests are implemented in simulation to assess the power tracking performance and conversion losses for the input tracking and the power tracking controller. In the first benchmark test the performance of the controllers given a slowly changing power reference is investigated. In the second test, the reaction to abrupt changes in the power reference is tested.

*1) Slow profile tracking:* In the first benchmark problem, the power at source 1 decreases at a rate of $-100$W per switching period. Source 3 consumes a constant power of $-1.5$kW, and source 2 compensates for the difference in power consumption and injection of the other sources. The simulation results are given in cycle periods $0 - 10$ in Fig. 5. It can be seen that for all cycle periods and both controllers the optimal solution for the desired power reference is reached in the second half of each cycle period as imposed by constraints (7d) and (7e). The small offset between the achieved and the reference power is due to the fact that the power in the control model is only an approximation of the actual power. As expected, the power tracking controller shows significantly better power tracking performance during the first half of each cycle than the simple input tracking controller. The input tracking controller still yields satisfactory power dynamics, for sources 1 and 2 the power transfer is lagging the desired power, resulting in a power tracking error that lies within the difference of the previous and the new reference. For source 3, the tracking behaviour is comparable to the power tracking controller. An important observation is that the improved power tracking performance of the power tracking controller comes at the

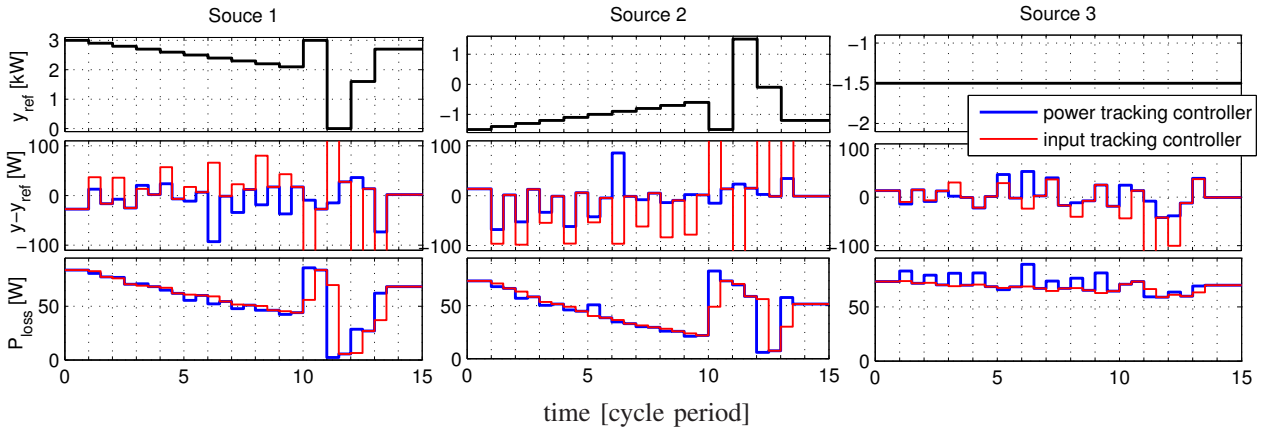


Fig. 5. Power tracking performance and resulting conversion losses for the input and power tracking controller at the different sources of the three-source DC-DC converter. Cycle periods $0-10$: slowly changing power reference. Cycle periods $10-15$: abruptly changing power reference.

cost of increased total system losses, i.e. the sum of the system losses at all sources.

*2) Abrupt profile tracking:* Starting from cycle period 10 in Fig. 5 the system experiences abrupt transitions in reference power at sources 1 and 2 at the beginning of every cycle period. The power at source 3 is kept constant.

As in the previous test, the power tracking controller achieves better power tracking. Due to limitations arising from the system dynamics, the system state cannot reach arbitrary values during a transition period. Thus the controller is not able to achieve perfect power tracking for such large changes in the power reference.

Despite the abrupt reference changes, the input tracking controller exhibits good overall power tracking performance. As in the previous benchmark problem, the transmitted power is lagging the reference for sources 1 and 2. For source 3 however a tracking error of up to $10\%$ of the desired power is observed. However, the input tracking controller still bears the advantage of lower system losses.

## VII. Conclusion

PWM systems do not yield a constant equilibrium for a given operating point but a cyclic steady state. The optimal cyclic steady state with respect to some cost criterion that features the switched dynamics of the system is obtained from an MIQP that cannot be solved in real-time. It is however possible to precompute the optimal cyclic steady states and store them in look-up tables for real-time implementation. To avoid adverse effects during transitions between precomputed cylclic steady states, additional measures have to be taken.

In this paper, a control approach for dynamic control of AC PWM systems whose system dynamics fulfill a set of given conditions has been introduced. The approach allows for transitions between the precomputed optimal cyclic steady state trajectories of different operating points within half a cycle, while avoiding adverse effects such as current displacement, high transition losses or transformer saturation.

The approach is applied to the class of multisource converters. It is verified in simulation for a three-source converter. Two optimal control problems are devised. One formulates input tracking and results in an input constrained QP that allows for real-time implementation of the resulting controller. The second optimal control problem additionally features output tracking. It results in an MIQP that cannot be solved in real-time, but is used to assess the performance of the simpler controller. In all the benchmark problems implemented in simulation, the input tracking controller achieves satisfactory performance. Furthermore, lower conversion losses are observed during transients. Hence, the proposed control approach is suitable for improving the dynamic performance of AC PWM systems.

## References


[1] S. Almér, S. Mariéthoz, and M. Morari, "Sampled Data Model Predictive Control of a Voltage Source Inverter for Reduced Harmonic Distortion," *IEEE Trans. on Control Systems Technology*, Sep. 2012.

[2] C. Fischer, S. Mariéthoz, and M. Morari, "Multisampled Hybrid Model Predictive Control Schemes for Pulse-Width Modulated Systems," in *IEEE Conf. on Decision and Control*, Orlando, Fl, USA, Dec. 2011.

[3] S. Mariéthoz and S. Almér, "Model predictive control," in *Dynamics and Control of Switched Electronic Systems*, ser. Advances in Indust. Control, F. Vasca and L. Iannelli, Eds. Springer, 2012, pp. 321–354.

[4] J. Rodriguez, P. Cortes, R. Kennel, and M. Kazrnierkowski, "Model predictive control – a simple and powerful method to control power converters," in *Power Electronics and Motion Control Conf., 2009. IPEMC '09. IEEE 6th International*, 2009, pp. 41–49.

[5] X. C. Ding, Y. Wardi, D. Taylor, and M. Egerstedt, "Optimization of switched-mode systems with switching costs," in *American Control Conf., 2008*, 2008, pp. 3965–3970.

[6] C. Fischer, S. Mariéthoz, and M. Morari, "An optimal modulation strategy for minimising the losses of isolated multisource DC-DC converters," in *IEEE IECON, Industrial Electronics Conf.*, Montreal, Canada, October 2012, pp. 2174–2179.

[7] S. Mariéthoz and A. Rufer, "Multisource DC-DC converter for the supply of hybrid multilevel converter," in *IEEE IAS, Industry Applications Conf.*, Tampa, FL, USA, October 2006, pp. 982 – 987.

[8] M. Kvasnica, P. Grieder, and M. Baotić, "Multi-Parametric Toolbox (MPT)," 2004. [Online]. Available: http://control.ee.ethz.ch/ mpt/

[9] J. Löfberg, "Yalmip : A toolbox for modeling and optimization in MATLAB," in *Proc. of the CACSD Conf.*, 2004.

[10] S. Richter, C. Jones, and M. Morari, "Computational complexity certification for real-time mpc with input constraints based on the fast gradient method," *Automatic Control, IEEE Trans. on*, vol. 57, no. 6, pp. 1391 –1403, June 2012.